JACS
JOURNAL OF THE AMERICAN CHEMICAL SOCIETY
Article
pubs.acs.org/JACS

Experimental and Theoretical Investigation of Molybdenum Carbide and Nitride as Catalysts for Ammonia Decomposition

Weiqing Zheng,[†] Thomas P. Cotter,[†] Payam Kaghazchi,[‡] Timo Jacob,[‡] Benjamin Frank,[†] Klaus Schlichte,[§] Wei Zhang,[†] Dang Sheng Su,*[,†,∥,⊥] Ferdi Schüth,[§] and Robert Schlögl[†]

[†]Department of Inorganic Chemistry, Fritz Haber Institute of the Max Planck Society, Faradayweg 4-6, 14195 Berlin, Germany

[‡]Institut für Elektrochemie, Universität Ulm, Albert-Einstein-Allee 47, 89069 Ulm, Germany

[§]Department of Heterogeneous Catalysis, Max Planck Institute for Coal Research, Kaiser-Wihelm-Platz 1, 45470 Mülheim an der Ruhr, Germany

[∥]Shenyang National Laboratory for Material Science, Institute of Metal Research, Chinese Academy of Sciences, 72 Wenhua Road, 110016 Shenyang, People's Republic of China

ABSTRACT: Constant CO_x-free H_2 production from the catalytic decomposition of ammonia could be achieved over a high-surface-area molybdenum carbide catalyst prepared by a temperature-programmed reduction−carburization method. The fresh and used catalyst was characterized by N_2 adsorption/desorption, powder X-ray diffraction, scanning and transmission electron microscopy, and electron energy-loss spectroscopy at different stages. Observed deactivation (in the first 15 h) of the high-surface-area carbide during the reaction was ascribed to considerable reduction of the specific surface area due to nitridation of the carbide under the reaction conditions. Theoretical calculations confirm that the N atoms tend to occupy subsurface sites, leading to the formation of nitride under an NH_3 atmosphere. The relatively high rate of reaction (30 mmol/((g of cat.) min)) observed for the catalytic decomposition of NH_3 is ascribed to highly energetic sites (twin boundaries, stacking faults, steps, and defects) which are observed in both the molybdenum carbide and nitride samples. The prevalence of such sites in the as-synthesized material results in a much higher H_2 production rate in comparison with that for previously reported Mo-based catalysts.

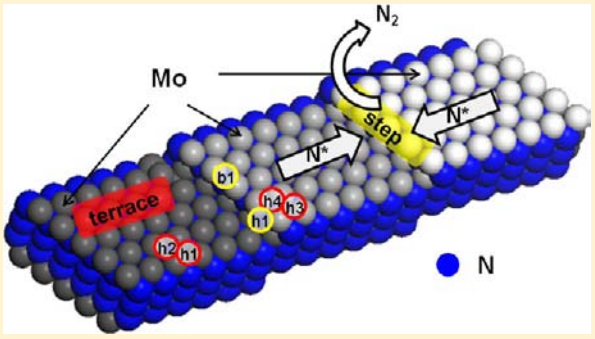

1. INTRODUCTION

Carbides and nitrides of early transition metals have been the focus of much attention following the pioneering work of Levy and Boudart,[1] who showed that tungsten carbides display Pt-like behavior in several catalytic reactions. It has been subsequently demonstrated that transition-metal carbides and nitrides are effective catalysts in a number of reactions that typically utilize group VIII noble metals as catalysts, including hydrogenation,[2] dehydrogenation,[3] hydrogenolysis,[4] isomerization,[1,5,6] and methane to syngas,[7] in which the catalytic activities approached or surpassed those of noble metals.

It is well-known that metal−nitrogen interactions play important roles in both the synthesis and decomposition of ammonia, since the adsorption and desorption of nitrogen are reaction-limiting steps for ammonia synthesis and decomposition, respectively.[8,9] Considering that the catalytic efficiency of the elements for the synthesis[10] and decomposition of ammonia has been correlated with the chemisorption energy of nitrogen, molybdenum carbides and nitrides have been applied in both the catalytic synthesis and decomposition of NH_3.[11] Oyama showed a number of interstitial alloys (molybdenum carbide and nitride) that were more active than ruthenium but less active than the doubly promoted iron catalyst for ammonia synthesis.[12] He also reported similar rate parameters for vanadium nitride to those of iron and platinum in ammonia decomposition.[13] Choi investigated vanadium carbide[14] and molybdenum carbide,[15] and Pansare et al. studied tungsten carbide[16] for ammonia decomposition. Those materials reported in the literature showed interesting performance for ammonia decomposition; unfortunately, none of the catalysts could achieve more than a 4 mmol/((g of cat.) min) H_2 formation rate, which is likely due to the low surface area of the reported materials.

One of the most facile routes to high-surface-area transition-metal carbides can be attributed to Lee et al.,[17] who developed a temperature-programmed reduction−carburization method which allows the formation of carbide materials from precursor oxides under a wide range of conditions. In this study, we prepared high-surface-area molybdenum carbide from *h*-MoO_3 metal oxide precursor using a temperature-programmed reduction−carburization under a flowing atmosphere of H_2 and CH_4.[18] This was applied in the catalytic decomposition of ammonia and exhibited high performance in H_2 production.

Received: October 2, 2012
Published: January 27, 2013

ACS Publications © 2013 American Chemical Society

dx.doi.org/10.1021/ja309734u | *J. Am. Chem. Soc.* 2013, 135, 3458−3464

2. EXPERIMENTAL SECTION

2.1. Preparation of Catalysts. The high-surface-area molybdenum carbide catalyst was synthesized via a temperature-programmed reduction−carburization of lab-made *h*-MoO_3 under a flowing atmosphere: a mixture of He, H_2, and CH_4 gases at 675 °C for 4 h.[18] The fresh molybdenum carbide is denoted as Mo_2C-fresh in this paper. In order to give a comparison between molybdenum carbide and noble metal ruthenium, 2 wt % Ru was deposited on graphite by the incipient wetness impregnation method.

2.2. Characterization Methods. Samples were analyzed by N_2 adsorption/desorption using a Quantachrome Autosorb AS-6B instrument and measured after a pretreatment under vacuum at 200 °C for 2 h. The specific surface areas were determined by applying the Brunauer−Emmet−Teller (BET) method using 11 points in the relative pressure p/p_0 range between 0.05 and 0.3. The pore size distributions were calculated using the Barrett−Joiner−Halenda (BJH) method from the desorption branch of the N_2 isotherm. Powder X-ray diffraction was carried out for all samples using a STOE STADI P diffractometer in transmission geometry (primary focusing Ge monochromator, Cu Kα1 radiation (λ = 1.5406 Å), linear position sensitive detector). The morphologies of all samples were investigated on a Hitachi S-5200 scanning electron microscope (SEM) coupled with an EDX detector for elemental analysis. The samples under investigation have been deposited on conducting carbon tape. All images were acquired using an acceleration voltage of 3 kV for better image contrast of surface features and 15 kV to investigate the inner cavities/subsurface of the samples. A transmission electron microscope (TEM) equipped with a FEG emitter (Philips CM200) and image energy filter (GIF200, Gatan) operated at 200 kV was used to perform overview and high-resolution (HRTEM) investigations for all samples. Electron energy-loss spectroscopy (EELS) spectra of all samples were acquired in diffraction mode at 0.1 eV per channel dispersion with a probe size of around 100 nm radius, circular region.

2.3. Catalytic Performance Measurement. All catalytic tests were conducted in the Department of Heterogeneous Catalysis at the Max-Planck-Institut für Kohlenforschung, Mülheim, Germany. Details of catalytic measurements: 50 mg of the catalyst was loaded in a quartz tube fixed bed reactor. Pure gaseous NH_3 (30 mL/min) was passed through the catalyst bed, and the temperature was increased to 600 °C with a ramp of 10 °C/min. The effluent gas was analyzed by an online gas chromatograph (MicroGC 3000A, Agilent) equipped with two lines, a PLOTU precolumn/Molsieve column combination with Ar as carrier gas for N_2, H_2, and CH_4 and a PLOTU column with He as carrier gas for NH_3 and CH_4. Both lines were equipped with TCD detectors. The apparent activation energy of Mo_2C was estimated by the Arrhenius equation ($E_a \equiv -R[((\partial \ln k)/(\partial(1)/(T)))]_P$, where R is the Boltzmann constant and k is the rate constant of ammonia decomposition at the temperature T) in the temperature region of 450−600 °C. The samples collected after 4 and 100 h of reaction are labeled as Mo_2C-NH_3-4h and Mo_2C-NH_3-100h, respectively.

2.4. Density Functional Theory Calculations. DFT calculations were performed using CASTEP[19] with Vanderbilt-type ultrasoft psedopotentials[20] and the generalized gradient approximation (GGA) exchange-correlation functional proposed by Perdew, Burke, and Ernzerhof (PBE).[21] A plane-wave basis set with an energy cutoff of 380 eV was used for all calculations. The Brillouin zones of the (1 × 1) surface unit cells of Mo_2C (0001) and MoN (0001) were sampled with 6 × 6 Monkhorst−Pack ***k***-point meshes. The surfaces were modeled with unsymmetric seven-layer slabs, where the lowest two layers were fixed at the bulk crystal structure. The geometries of the remaining layers were optimized to <0.03 eV/Å.

3. RESULTS AND DISCUSSION

3.1. Catalytic Performance of High-Surface-Area Molybdenum Carbide. Catalytic NH_3 decomposition was conducted according to the procedure detailed in the Experimental Section. The performance of Mo carbide over 100 h on stream at 600 °C is shown in Figure 1. Here the NH_3 conversion of the fresh high-surface-area Mo_2C decreases from 85% to 71% over 15 h and subsequently stabilizes at a constant H_2 formation rate of about 30 mmol/((g of cat.) min). The catalytic activity of 2 wt %Ru/graphite is also shown in Figure 1 for comparison, showing an H_2 formation rate of about 37 mmol/((g of cat.) min) under the same conditions. The apparent activation energy for the decomposition of NH_3 over Mo_2C (as measured from 600 to 450 °C, calculated according to the Arrhenius equation) is about 89 kJ/mol, which compares favorably to the value found for 2 wt % Ru supported on different carbon materials (75−85 kJ/mol).[22] These findings imply that the high-surface-area transition-metal carbides have the potential to replace noble metals in the application for CO_x-free H_2 production from ammonia. Owing to the high reaction temperatures the reaction process is likely beyond kinetic control: i.e., influenced by mass transfer limitation. However, considering the low surface areas of the catalysts, the internal diffusion effects are less pronounced as for high-surface-area materials.

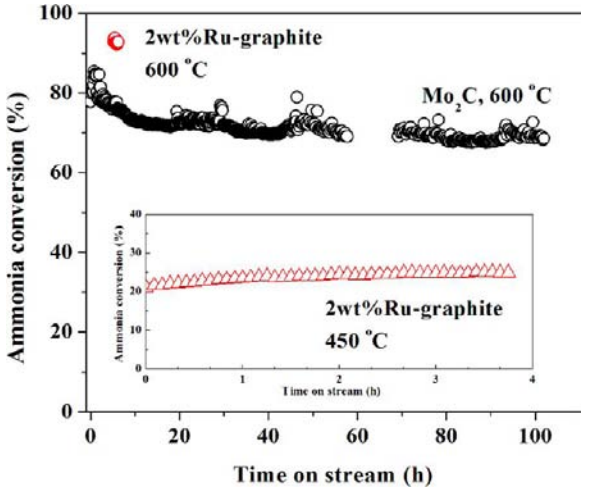

Figure 1. Catalytic activity and stability of (circles) Mo carbide and (triangles) graphite-supported 2 wt % Ru catalyst for NH_3 decomposition. Reaction conditions: 50 mg of the sample, NH_3 space velocity 36000 mL/((g of cat.) min), reaction temperature 600 °C (Mo) or 450 °C (Ru).

3.2. Characterizations. The results of the physico-structural characterizations of the fresh and used (4 and 100 h) catalysts are summarized in Table 1. Figure 2 shows the N_2 physisorption isotherms and BJH pore size distributions for the desorption branches of all samples. The isotherm of the fresh molybdenum carbide sample is intermediate between type II and type IV, according to the IUPAC classification,[31] with an H3 hysteresis loop indicating a slitlike mesopore structure. As shown in Figure 2b, two different pore-size distributions (2−4

Table 1. Physical Properties of Samples

sample	BET surface area[a] (m^2/g)	pore volume[b] (10^{-2} cm^3/g)	phase structure[c]
Mo_2C	47.7	8.9	hexagonal Mo_2C
Mo_2C-NH_3-4h	6.0	4.6	hexagonal Mo_2C and MoN
Mo_2C-NH_3-100h	4.8	2.6	hexagonal MoN

[a]Calculated from N_2 adsorption and desorption analysis. [b]Total pore volume. [c]determined from XRD and TEM analysis

dx.doi.org/10.1021/ja309734u | J. Am. Chem. Soc. 2013, 135, 3458−3464

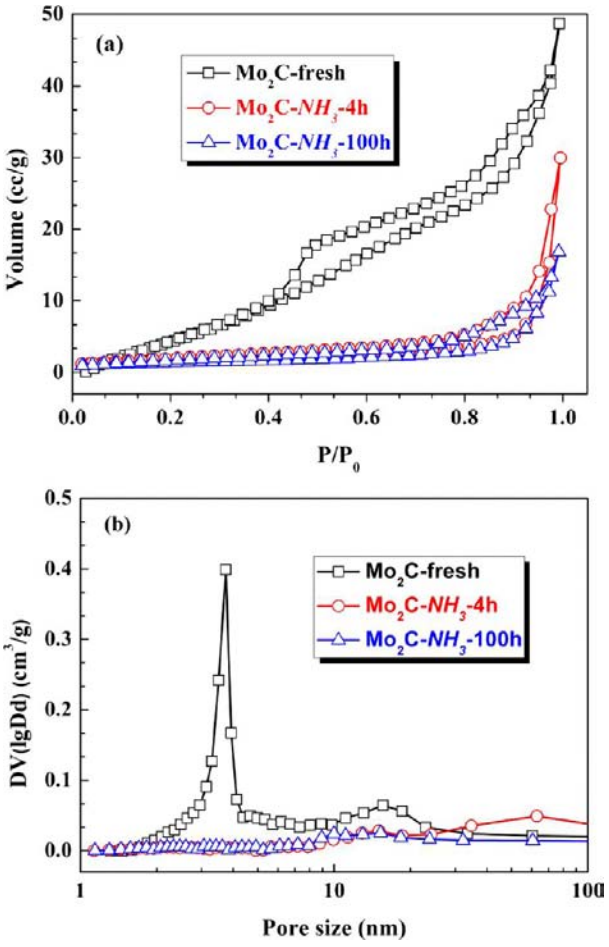

Figure 2. N_2-adsorption/desorption analysis: (a) isotherms; (b) pore size distribution from BJH desorption.

and 10−11 nm) were observed for the fresh Mo_2C. Following ammonia decomposition for 4 h at 600 °C, the mesopores between 2 and 4 nm were not observed, and the isotherm changed to a typical type II shape, indicating the disappearance of the mesopore structure. This resulted in a considerable drop of surface area from 50 to 6 m^2/g. The surface area and mesopore structures further decreased with time on stream (TOS). After 100 h of reaction, there was about 90% loss of surface area. However, the loss of catalytic activity was only about 15%. Therefore, in order to find an agreement between the solid materials and catalytic performance, further characterizations of the Mo_2C, Mo_2C-NH_3-4h, and Mo_2C-NH_3-100h catalysts were carried out.

The morphologies of all the samples were investigated by transmission/scanning electron microscopy (SEM and TEM). Figure 3 shows representative TEM images of the three samples. As shown in Figure 3a, the fresh Mo_2C sample has a homogeneous mesopore structure, giving the uniform distribution of the bright regions in the TEM image. After reaction for 4 h, the catalyst appears to lose the porosity (TEM image of Figure 3b). Further, very few mesopores can be observed in the sample of Mo_2C-NH_3-100h (in Figure 3c), which has increased in apparent density by comparison with the fresh sample. These observations are in good agreement with the results obtained from N_2 physisorption. The representative SEM images with different magnifications of all samples shown in Figure 4 also agree with the findings that, after reaction of ammonia

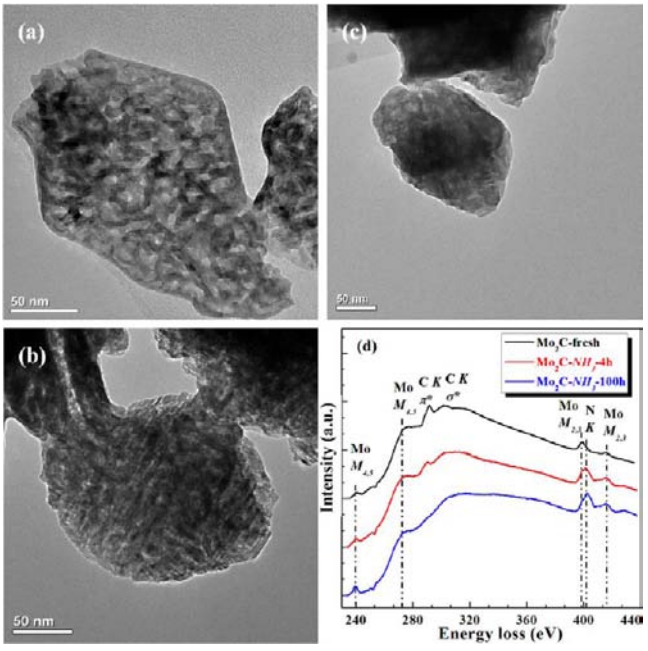

Figure 3. TEM images and EELS spectra of fresh and 4 and 100 h used Mo carbide/nitride samples: (a) Mo_2C-fresh; (b) Mo_2C-NH_3-4h; (c) Mo_2C-NH_3-100h; (d) Mo M-edge, C and N K-edge EELS spectra of the samples.

decomposition, the catalyst became a more compact solid structure with lower specific surface area.

Both powder XRD and high-resolution TEM techniques were used to identify the phases of molybdenum carbide and nitride and compare them with various phases of these materials reported in the literature.[23,24] Figure 5 shows the

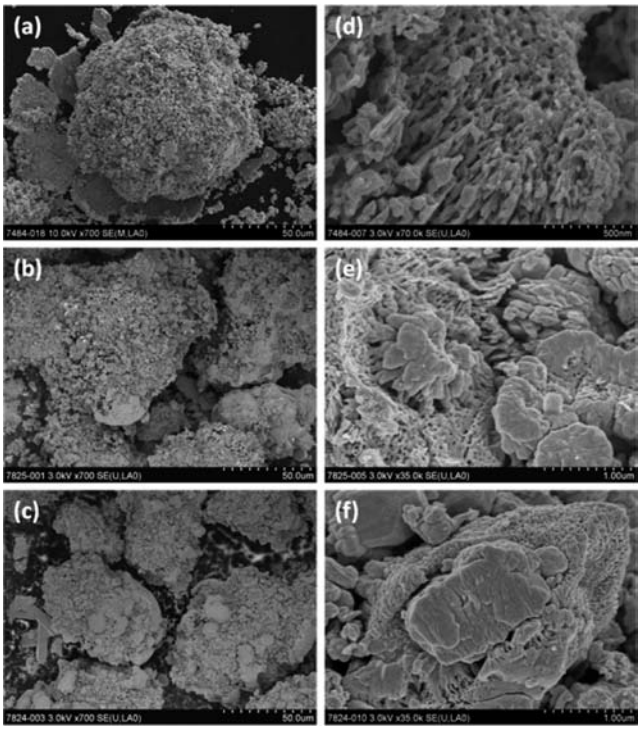

Figure 4. SEM images of samples: (a, d) Mo_2C-fresh; (b, e) Mo_2C-NH_3-4h; (c, f) Mo_2C-NH_3-100h.

dx.doi.org/10.1021/ja309734u | J. Am. Chem. Soc. 2013, 135, 3458−3464

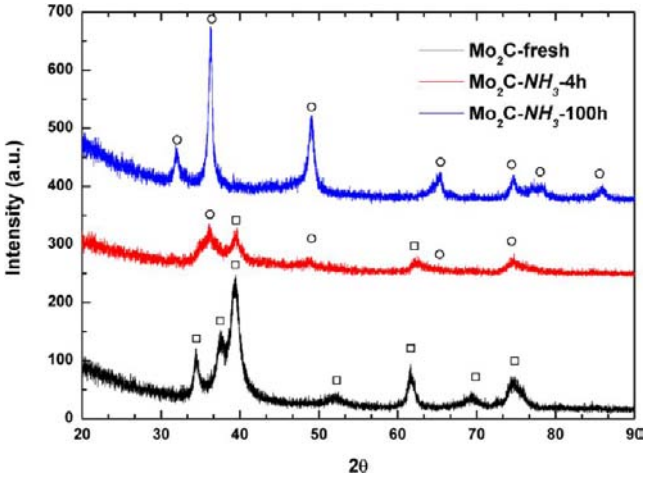

Figure 5. XRD patterns of fresh and 4 and 100 h used Mo carbide samples: (squares) JCPD Mo_2C; (circles) JCPD MoN. All used samples were collected after the ammonia decomposition reaction and sealed under the protection of inert gas.

XRD patterns of the fresh and used samples. The XRD pattern of the fresh Mo_2C sample indicates a hexagonal-close-packed structure (β-Mo_2C), which was compared with the reference pattern of JCPD-00-035-0787 Mo_2C (34.4° (100), 38.0° (002), 39.4° (101), 61.5° (103), and 74.6° (112)). The XRD pattern of used molybdenum carbide collected after 100 h indicated a hexagonal MoN structure by comparinson with JCPD-01-089-5024 MoN (31.8° (002), 36.1° (200), 48.8° (202), 64.9° (220), 78.0° (204), and 85.3° (402)). Both β-Mo_2C and δ-MoN diffraction peaks can be observed in the pattern of Mo_2C-NH_3-4h, which indicates nitridation of Mo_2C during the ammonia decomposition reaction. The XRD pattern of Mo_2C-NH_3-4h exhibited broader and lower intensity in comparison to Mo_2C-fresh and Mo_2C-NH_3-100h, indicating smaller crystallites of both Mo_2C and MoN. We assume that the nitridation of the carbide is initiated at dislocation structures in the primary carbide crystallites, which act as nucleation sites for continuously growing MoN crystallites.

Figure 6 shows the high-resolution TEM images of the fresh and used catalysts, revealing the polycrystalline structures of all the samples. Various lattice fringes and analysis of their characteristic acute angles confirmed that there is only one phase in either the fresh or 100 h used sample: that is, β-Mo_2C (Mo_2C-fresh) and δ-MoN (Mo_2C-NH_3-100h), respectively. Both of these two structures can be observed coexisting in the Mo_2C-NH_3-4h sample (Figure 6b). In addition, as shown in the inserted images in Figure 6, a large number of twin boundaries, stacking faults, steps, and defects could be observed among the high-resolution images of all the observed samples, which can be recognized as highly energetic sites in these samples.[25]

In a catalytic cycle which involves several elementary steps, the step which is not in thermodynamic equilibrium is the rate-determining step. In ammonia synthesis this step is the dissociative chemisorption of nitrogen.[26] In the reverse reaction, ammonia decomposition, this step is the recombinative desorption of dinitrogen atoms from the surface. It was reported[8] that in ammonia synthesis the active site might occur on a single step edge, as the required hydrogen populates the terraces of metal particles in a highly mobile form. Instead, the active site for the reverse reaction, ammonia decomposition, is a larger ensemble than that for synthesis. Unlike the ammonia

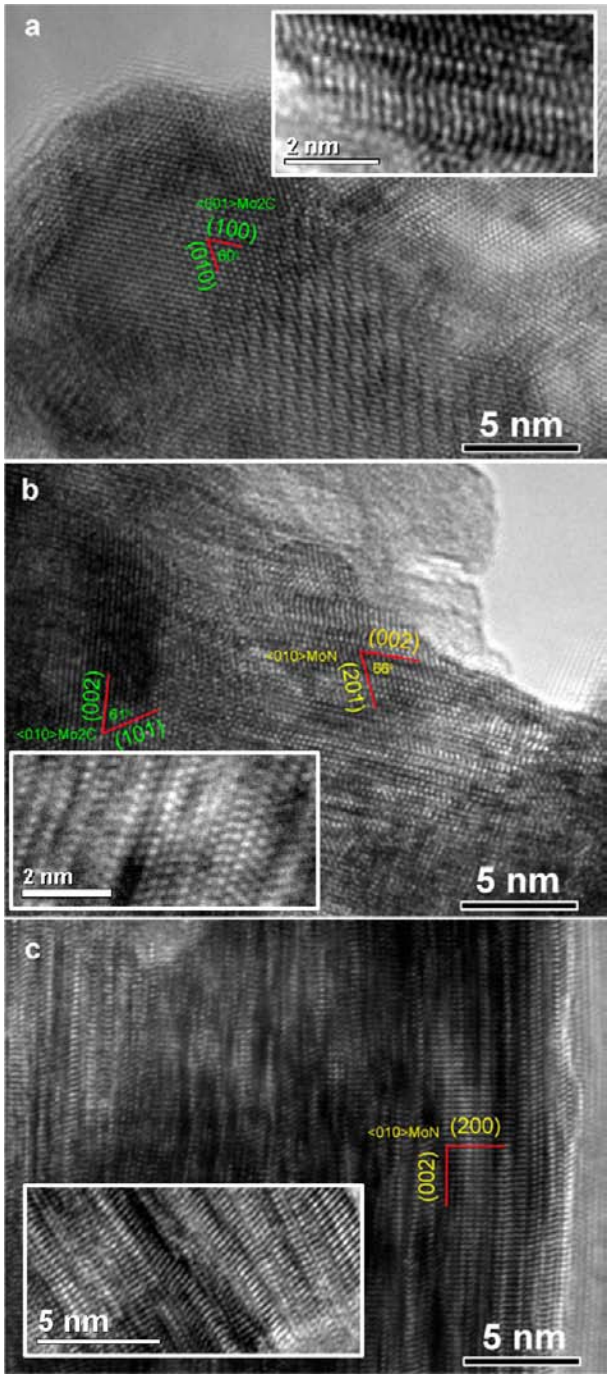

Figure 6. High-resolution images of fresh and used molybdenum carbide samples indexing with different lattice orientations: (a) Mo_2C-fresh; (b) Mo_2C-NH_3-4h; (c) Mo_2C-NH_3-100h.

synthesis, two neighboring step sites will be needed for the formation of the N−N bond. Additional terrace sites might also be needed for H atoms due to the inhibition effect of hydrogen. As a bulk solid system, the carbides and nitrides in this study strongly differ from supported metal nanoparticles, which expose much more specific surface area for reactant chemisorption. Nor is this the model catalyst or single crystal of surface science, both of which could only offer one or several coordination structures. We believe that high-energy sites related to dislocation defects and crystal twinning, which are observed in these carbide and nitride samples, could be the

dx.doi.org/10.1021/ja309734u | J. Am. Chem. Soc. 2013, 135, 3458−3464

active sites for ammonia decomposition. This may explain why the significant drop of the specific surface area did not cause a dramatic decrease in catalytic performance.

Electron energy-loss spectroscopy (EELS) is a suitable technique for the chemical analysis of transition-metal carbides and nitrides.[27] Unfortunately, however, the Mo $M_{4,5}$-edge (at ca. 227 eV) and $M_{2,3}$-edge (doublet peaks at ca. 410 and 392 eV, respectively) overlap with the C K-edge (at ca. 284 eV) and N K-edge (at ca. 401 eV), causing difficulty in the standard procedure for EELS analysis.[28] Figure 3d summarizes the EELS spectra of all samples. In the spectra of Mo_2C-fresh, the Mo M-edge is broad and has small features at ca. 227, 393, and 410 eV, respectively. A large peak was observed for the C K-edge which is indicative of the presence of sp^2-bonded carbon.

After 4 h of reaction, the intensity of the carbon peak decreases while the formation of N K-edge at ca. 401 eV is observed, consistent with the formation of molybdenum nitride. After 100 h, nearly no carbon edge is observed, indicating the complete nitridation of molybdenum carbide. In ammonia synthesis, the dissociative adsorption of nitrogen on metallic surfaces leads to a state of adsorbed nitrogen atoms sometimes referred to as "nitride"; the dissolved nitrogen can not only recombine and desorb but also be dissolved in the subsurface and form a solid solution.[8] In ammonia decomposition, after cleavage of the N−H bond, the adsorbed N atoms may also undergo the same phenomena as seen in ammonia synthesis to form the "surface" and "subsurface" nitride and further form the bulk nitride. At the same time, the adsorbed H atoms can not only recombine and desorb but also react with carbon atoms in solid solution to form C−H bonds and eventually desorb from the surface as CH_4. In Figure 7a, the EELS spectra of the Mo_2C-NH_3-4h sample is shown, which has both Mo_2C and MoN structures, as confirmed by XRD and TEM analysis. Two representative areas were selected to measure the EELS spectra. One is on the outer perimeter of the selected particle, which could more or less be regarded as the "surface" of the sample; the other is in the center of the selected particle, which is close to the "bulk" region. The intensity of carbon features of the "bulk" area is much more pronounced than the "surface" part, which contains nearly no C signal. These results indicated the nitridation of Mo_2C during ammonia decomposition starting from the surface to the bulk, which is in good agreement with previous characterization and also with the literature.[8]

3.3. Theoretical Calculations. We first determined the heats of formation of different Mo−C−N bulk compounds. In addition to the experimentally known *hexa*-Mo_2C (space group $P6_3/mmc$ (No. 194))[29] and *δ1*-MoN (space group $P\bar{6}m2$ (No. 187))[30] structures, we constructed Mo_2C_2, Mo_2CN, and Mo_2N_2 by adding C and N atoms to interstitial sites of *hexa*-Mo_2C. As can be seen in Figure 8, the nitrided structures are more stable than carbide structures by roughly 0.2 eV per unit cell, showing that there is a driving force for molybdenum carbide to convert into a nitride under a nitrogen atmosphere. Although we find that a mixed Mo_2CN crystal phase should even be more stable than Mo_2N_2 and MoN, its formation might be kinetically hindered, since at the real reaction conditions the surface is likely saturated with adsorbed N atoms, which could force the formation of nitride.

The rate-limiting steps for both the synthesis (N_2 dissociation) and decomposition (recombinative desorption of N atoms) of ammonia are related to the interaction between N and active surface sites of the catalyst. Also, it was reported

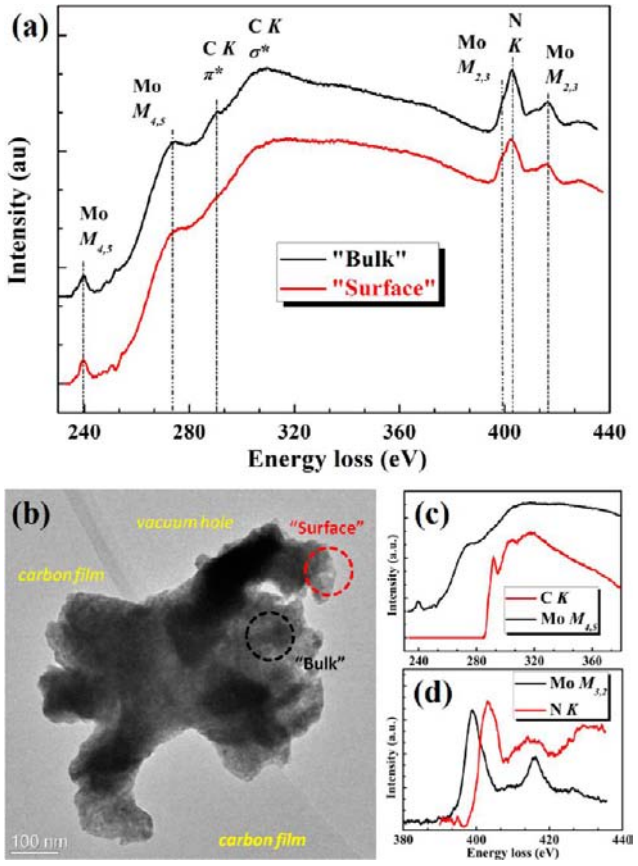

Figure 7. (a) EELS spectra of the Mo_2C-NH_3-4h sample with two different selective areas, (b) TEM image of the Mo_2C-NH_3-4h sample labeled with two probe areas for EELS measurements, and (c, d) reference spectra of carbon K-edge and molybdenum $M_{4,5}$-edge and nitrogen K-edge and molybdenum $M_{3,2}$-edge. respectively.

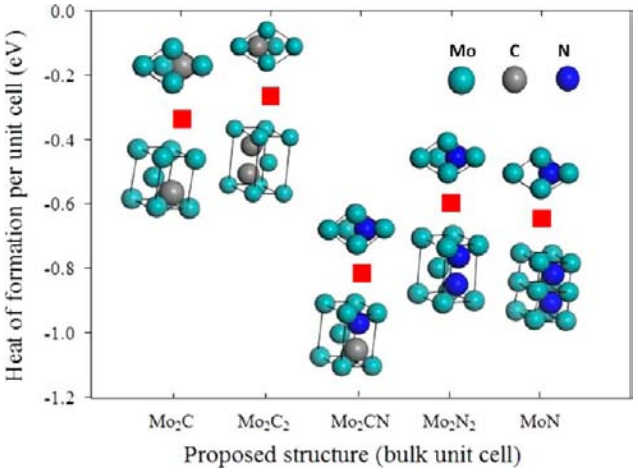

Figure 8. Calculated heat formation of different unit cells of molybdenum carbide and nitride structures.

that the computed TOFs on the metal surface of ammonia synthesis could be perfectly correlated with the computed heats of chemisorptions of activated nitrogen by the link between the kinetic parameters of a reaction with the thermodynamic parameters of bond strengths of adsorbates.[8,10,31] It was further reported that the catalytic performance of ammonia decomposition on the bimetallic surface can be predicted from the binding energies of N-metal from DFT calculations guided

dx.doi.org/10.1021/ja309734u | J. Am. Chem. Soc. 2013, 135, 3458−3464

from first-principles-based microkinetic models.[32] Therefore, we concentrated on the bond strengths between N and the catalyst surface, which should play the dominant role in both the synthesis and decomposition of ammonia. We conducted a series of calculations for nitrogen adsorption on stepped *hexa*-$Mo_2C(0001)$ and *δ1*-MoN(0001), which are comparable to the catalysts' structures proposed by the experimental findings. Both surfaces were modeled as stepped surfaces with six atom-wide terraces of (0001) orientation, separated by double-atomic steps in the case of $Mo_2C(0001)$ and monatomic steps in case of *δ1*-MoN(0001). Nonequivalent bridge (b) and hollow (h) sites near the step (yellow circles in Figure 9) or on the terrace (red circles in Figure 9) are considered.

The binding energies that were calculated by subtracting the total energy of the clean surface and half of a N_2 molecule in the gas phase from the total energy of the surface with nitrogen are shown in Figure 9. On both stepped surfaces, N prefers binding at the step edges, where the calculated binding energies are 0.81 and 0.35 eV larger in comparison to binding at terrace sites of $Mo_2C(0001)$ or *δ1*-MoN(0001), respectively. This can be understood by the fact that nitrogen atoms have three unpaired electrons and prefer high coordination sites. Following the previous discussion on the role of the binding energies, the lower heats of chemisorption of N may thus indicate an increased activity for ammonia decomposition. For Mo_2C, since N adsorption is much more favorable (by ∼0.85 eV) at the step sites than on the terrace sites, the decomposition of NH_3 most likely only occurs at steps. For MoN, the difference in the binding energy at the step and terrace sites is only ∼0.35 eV, which might show that the reaction can occur at steps as well as over terraces. Therefore, although the binding energy of N is stronger over MoN than over Mo2C, we expect the former to be more active because of a greater number of active sites. While the previous studies already show the general activity trend, it will be the aim of future work to elucidate the full reaction mechanism on the different surfaces to allow for quantitative conclusions of their activities.

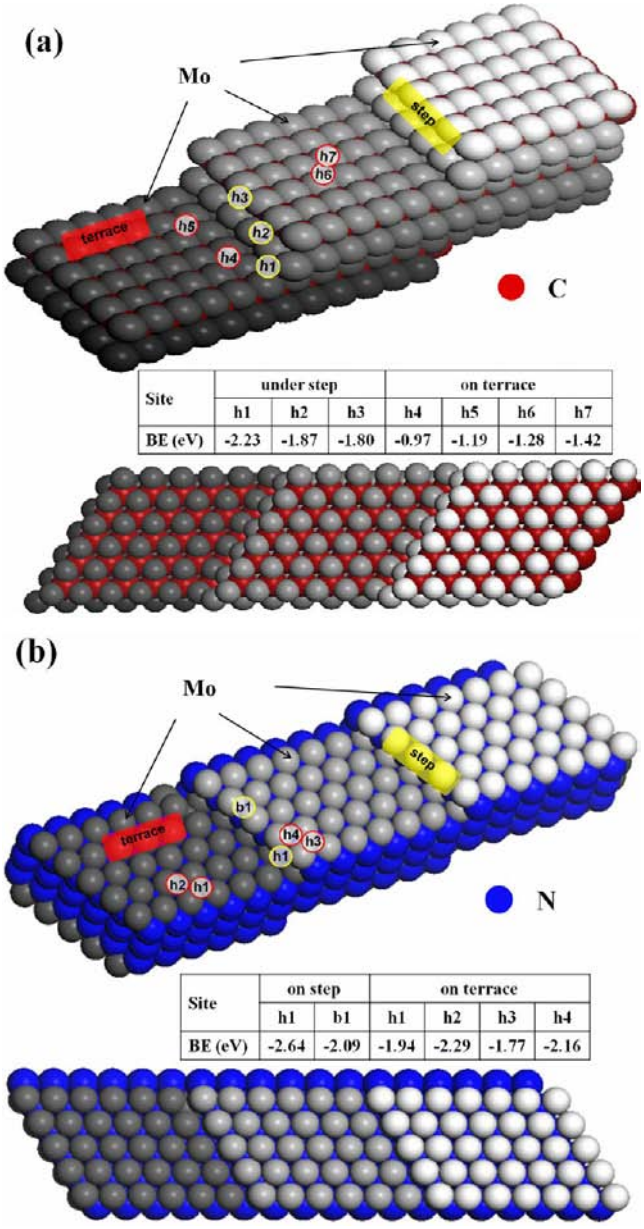

Site	under step			on terrace			
	h1	h2	h3	h4	h5	h6	h7
BE (eV)	-2.23	-1.87	-1.80	-0.97	-1.19	-1.28	-1.42

Site	on step		on terrace			
	h1	b1	h1	h2	h3	h4
BE (eV)	-2.64	-2.09	-1.94	-2.29	-1.77	-2.16

Figure 9. Calculated nitrogen adsorption energies (binding energy (eV) referenced to $^1/_2$ N_2 molecule) at different sites on terraces and steps of $Mo_2C(0001)$ and MoN(0001). Labels h and b indicate hollow and bridge sites, respectively.

4. CONCLUSIONS

In summary, we reported a high-performance ammonia decomposition catalyst of high-surface-area molybdenum carbide, which could achieve about 30 mmol/((g of cat.) min) constant H_2 production rate. The comprehensive characterization of fresh and used samples showed that the high-surface-area Mo_2C not only can crack the NH_3 molecule but also has a tendency to form MoN under a pure ammonia atmosphere at high temperature (600 °C), causing a significant drop of specific surface area (from about 50 m^2/g to about 5 m^2/g). Theoretical calculations showed that the N atoms tend to assume subsurface positions of Mo_2C, promoting the progressive formation of a molybdenum nitride. This result is in agreement with the EELS analysis over the sample collected after 4 h of reaction: that is, MoN is dominant on the surface compared to the bulk.

Over 100 h of catalytic measurements the activity was observed to drop by about 15% over the first 20 h before stabilizing. This drop in activity is not proportional to the drop in specific surface area, indicating that the molybdenum nitride may be more active for ammonia decomposition in comparison to molybdenum carbide. The opposite order was observed by Oyama over *β*-Mo_2C and *γ*-Mo_2N for ammonia synthesis at 400 °C.[12] We believe that the abundance of highly energetic sites (twin boundaries, stacking faults, steps, and defects) observed on molybdenum nitride should be the most active sites for cracking ammonia, since this reaction requires high electron density as well as undercoordinated sites to proceed. The observation of N−catalyst interactions over the terrace and step locations of Mo_2C and MoN showed the importance of high-energy sites for ammonia decomposition, in agreement with earlier studies in the literature.[33] N atoms tend to be more strongly bound (0.4 eV higher) to the step edge on MoN(0001) than on $Mo_2C(0001)$, which likely benefits the difficult step of N−N recombination through surface diffusion from two sites of ammonia cleavage on weakly adsorbing sites (terraces).[8]

dx.doi.org/10.1021/ja309734u | J. Am. Chem. Soc. 2013, 135, 3458−3464

AUTHOR INFORMATION

Corresponding Author

E-mail: dangsheng@fhi-berlin.mpg.de.

Present Address

[⊥]Shenyang National Laboratory for Material Science, Institute of Metal Research, Chinese Academy of Sciences, 72 Wenhua Road, 110016, Shenyang, People's Republic of China. E-mail: dssu@imr.ac.cn.

Notes

The authors declare no competing financial interest.

ACKNOWLEDGMENTS

We gratefully acknowledge technical assistance from Dr. Bo Zhu, Gisela Weinberg, Gisela Lorenz, and Edith Kitzelmann at the Fritz Haber Institute of the Max Planck Society. The Ulm group gratefully acknowledges support from the "Bundesministerium für Bildung und Forschung" (BMBF) and the European Union through the ERC-Starting Grant THEOFUN. This work was financially supported by the EnerChem project of the Max Planck Society.

REFERENCES

(1) Levy, R. B.; Boudart, M. *Science* **1973**, *181*, 547−549.
(2) Patterson, P. M.; Das, T. K.; Davis, B. H. *Appl. Catal., A* **2003**, *251*, 449−455.
(3) Leclercq, L.; Provost, M.; Pastor, H.; Leclercq, G. *J. Catal.* **1989**, *117*, 384−395.
(4) Neylon, M. K.; Choi, S.; Kwon, H.; Curry, K. E.; Thompson, L. T. *Appl. Catal., A* **1999**, *183*, 253−263.
(5) Ribeiro, F. H.; Dalla Betta, R. A.; Boudart, M.; Baumgartner, J.; Iglesia, E. *J. Catal.* **1991**, *130*, 86−105.
(6) Bouchy, C.; Pham-Huu, C.; Heinrich, B.; Chaumont, C.; Ledoux, M. J. *J. Catal.* **2000**, *190*, 92−103.
(7) Claridge, J. B.; York, A. P. E.; Brungs, A. J.; Marquez-Alvarez, C.; Sloan, J.; Tsang, S. C.; Green, M. L. H. *J. Catal.* **1998**, *180*, 85−100.
(8) Schlögl, R. In *Handbook of Heterogeneous Catalysis*; Ertl, G., Knözinger, H., Schüth, F., Weitkamp, J., Eds.; Wiley-VCH: Weinheim, Germany, 2008; Vol. *12*.
(9) Schlögl, R. *Angew. Chem., Int. Ed.* **2003**, *42*, 2004−2008.
(10) Logadottir, A.; Rod, T. H.; Nørskov, J. K.; Hammer, B.; Dahl, S.; Jacobsen, C. J. H. *J. Catal.* **2001**, *197*, 229−231.
(11) Kojima, R.; Aika, K.-i. *Appl. Catal., A* **2001**, *219*, 141−147.
(12) Oyama, S. T. *Catal. Today* **1992**, *15*, 179−200.
(13) Oyama, S. T. *J. Catal.* **1992**, *133*, 358−369.
(14) Choi, J.-G. *J. Catal.* **1999**, *182*, 104−116.
(15) Choi, J.-G. *J. Ind. Eng. Chem.* **2004**, *10*, 967−971.
(16) Pansare, S.; Torres, W.; Goodwinjr, J. *Catal. Commun.* **2007**, *8*, 649−654.
(17) Lee, J. S.; Oyama, S. T.; Boudart, M. *J. Catal.* **1987**, *106*, 125−133.
(18) Cotter, T. P. *Thesis*, Fritz-Haber-Institut der Max-Planck Gesellschaft, 2011.
(19) Segall, M. D.; Lindan, P. J. D.; Probert, M. J.; Pickard, C. J.; Hasnip, P. J.; Clark, S. J.; Payne, M. J. *J. Phys. Condens. Mater.* **2002**, *14*, 2717.
(20) Vanderbilt, D. *Phys. Rev. B* **1990**, *41*, 7892.
(21) Perdew, J. P.; Burke, K.; Ernzerhof, M. *Phys. Rev. Lett.* **1996**, *77*, 3865.
(22) Zheng, W.; Zhang, J.; Zhu, B.; Blume, R.; Zhang, Y.; Schlichte, K.; Schlögl, R.; Schüth, F.; Su, D. S. *ChemSusChem* **2010**, *3*, 226−230.
(23) Hugosson, H. W.; Eriksson, O.; Nordstrom, L.; Jansson, U.; Fast, L.; Delin, A.; Wills, J. M.; Johansson, B. *J. Appl. Phys.* **1999**, *86*, 3758−3767.
(24) Perry, A. J.; Baouchi, A. W.; Petersen, J. H.; Pozder, S. D. *Surf. Coat. Technol.* **1992**, *54*−*55*, 261−265.
(25) Somorjai, G. A.; Li, Y. *Introduction to Surface Chemistry and Catalysis*; Wiley: New York, 2010.
(26) Ertl, G. *Catalytic Ammonia Synthesis*; Springer: New York, 1991.
(27) Kuimalee, S.; Chairuangsri, T.; Pearce, J. T. H.; Edmonds, D. V.; Brown, A. P.; Brydson, R. M. D. *Micron* **2010**, *41*, 423−429.
(28) Egerton, R. F. *Electron Energy-Loss Spectroscopy in the Electron Microscope*, 2nd ed.; Springer: New York, 1996.
(29) Clougherty, E. V.; Lothrop, K. H.; Kafalas, J. A. *Nature* **1961**, *191*, 1194−1194.
(30) Kanoun, M. B.; Goumri-Said, S.; Jaouen, M. *Phys. Rev. B* **2007**, *76*, 134109.
(31) Jacobsen, C. J. H.; Dahl, S.; Clausen, B. S.; Bahn, S.; Logadottir, A.; Nørskov, J. K. *J. Am. Chem. Soc.* **2001**, *123*, 8404−8405.
(32) Hansgen, D. A.; Vlachos, D. G.; Chen, J. G. *Nat. Chem.* **2010**, *2*, 484−489.
(33) Dahl, S.; Logadottir, A.; Jacobsen, C. J. H.; Nørskov, J. K. *Appl. Catal., A* **2001**, *222*, 19−29.